Supplementary Material A

The parameter identification method

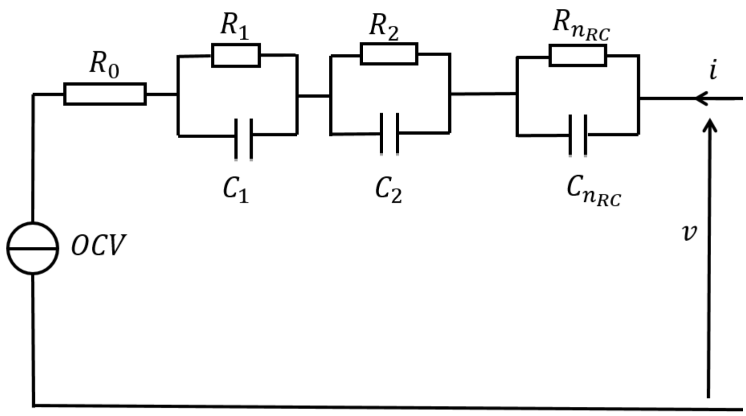

Figure S 1 Battery equivalent circuit network (ECN)

In the electrical ECN model shown in Figure S 1, v and i represent the ECN terminal voltage and current, respectively. Denote n_{RC} as the number of resistor-capacitor (RC) branches and define v_j, i_j ($j = 1, 2 \cdots n_{\mathrm{RC}}$) as the voltage drop and current through resistance R_j, and $v_j = R_j i_j$. The time constant is $\tau_j = R_j C_j$. The current i and the RC parameters are assumed to be constant between two measurement samples so that

$$v_j(k+1) = a_j v_j(k) + R_j(1-a_j)i(k), \quad j = 1,2,\ldots,n_{RC}, \tag{1}$$

where

$$a_j = exp(-t_s/\tau_j), \tag{1}$$

and $i_j(k)$ stands for current i_j at the *k*-th sampling time. t_s is sampling interval of time (unit: second). Using the widely employed coulomb counting method [1], [2], the battery State of Charge (*SoC*) is written as

$$SoC(k+1) = SoC(k) + \frac{t_s}{3600C_n} i(k), \tag{2}$$

where C_{n} is the battery nominal capacity at 25 °C (unit: Ampere-hour). The battery terminal voltage can be expressed as

$$v(k) = OCV(SoC(k)) + R_0 i(k) + \sum_{j=1}^{n_{RC}} v_j(\mathrm{k}) \tag{3}$$

The batteries were tested under the full SoC range (from 100% to end of discharge), at 5 temperature levels ([15, 25, 35, 45, 55] °C) and two current rates ([1C, 2C]). The RC time constants were set as constant. This can noticeably reduce the parameter optimisation complexity without sacrificing the model accuracy [3]. On the other hand, the dependency of battery internal resistance on SoC, temperature (T) and current rates (I), is captured using a 3D look-up table.

The breakpoints of SoC, temperature and current of the 3D look-up table are set as follows,

$$0 \leq SoC_1 < SoC_2 < \ldots < SoC_{n_{soc}} \leq 100\%, \tag{4}$$

$$T_1 = 15°\mathrm{C}, T_2 = 25°\mathrm{C}, T_3 = 35°\mathrm{C}, T_4 = 45°\mathrm{C}, T_5 = 55°\mathrm{C}$$

$$I_1 = 5A, I_2 = 10A$$

The resistor dependency on SOC, T and I is described as follows,

$$R_j(SoC, T, i) = \sum_{k_{SoC}=1}^{n_{SoC}} \sum_{k_T=1}^{5} \sum_{k_I=1}^{2} R_{j,k_{SoC},k_T,k_I} f_{k_{SoC},k_T,k_I}(SoC, T, i)\,, j = 0,1, \ldots, n_{RC}, \tag{6}$$

Where R_{j,k_{SoC},k_T,k_I} is the value of R_j at the node of the 3D look-up table ($SoC = SoC_{k_{SoC}}, T = T_{k_T}, i = I_{k_I}$), and $f_{k_{SoC},k_T,k_I}(SoC, T, i)$ is the base function,

$$f_{k_{SoC},k_T,k_I}(SoC, T, i) = FS_{k_{SoC}}(SoC) FT_{k_T}(T) FI_{k_I}(i)$$

Where the SoC-based look-up function is defined as follows,

$$FS_1(SoC) = \begin{cases} 1, & if\ SoC \leq SoC_1 \\ \dfrac{SoC_2 - SoC}{SoC_2 - SoC_1}, & if\ SoC_1 < SoC < SoC_2 \end{cases}$$

$$FS_m(SoC) = \begin{cases} \frac{SoC - SoC_{m-1}}{SoC_m - SoC_{m-1}}, & if\ SoC_{m-1} \leq SoC < SoC_m \\ \frac{SoC_{m+1} - SoC}{SoC_{m+1} - SoC_m}, & if\ SoC_m \leq SoC < SoC_{m+1} \end{cases}, \ \mathrm{m} = 2, \ldots, n_{soc} - 1, \tag{7}$$

$$FS_{n_{soc}}(SoC) = \begin{cases} \dfrac{SoC - SoC_{n_{soc}-1}}{SoC_{n_{soc}} - SoC_{n_{soc}-1}}, & if\ SoC_{n_{soc}-1} \leq SoC < SoC_{n_{soc}} \\ 1, & if\ SoC_{n_{soc}} \leq SoC \end{cases}$$

The temperature-based look-up function is defined as follows,

$$FT_1(T) = \frac{T_2 - T}{T_2 - T_1}, if\ T \leq T_2$$

$$FT_m(T) = \begin{cases} \frac{T - T_{m-1}}{T_m - T_{m-1}}, & if\ T_{m-1} \leq T < T_m \\ \frac{T_{m+1} - T}{T_{m+1} - T_m}, & if\ T_m \leq T < T_{m+1} \end{cases}, \ \mathrm{m} = 2, \ldots, 4, \tag{8}$$

$$FT_5(T) = \frac{T - T_4}{T_5 - T_4}, \qquad if\ T_4 \leq T$$

Finally, the current based look-up function is defined as follows,

$$FI_1(i) = \frac{i - I_2}{I_1 - I_2}, \qquad if\ i \leq I_2 \tag{9}$$

$$FI_2(i) = \frac{i - I_1}{I_1 - I_1}, \qquad if\ I_1 \leq i$$

Substitute Eq(1), Eq(6) into Eq(4), yielding

$$v_j(k+1) = a_j v_j(k) + \sum_{k_{SoC}=1}^{n_{SoC}} \sum_{k_T=1}^{5} \sum_{k_I=1}^{2} R_{j,k_{SoC},k_T,k_I} f_{k_{SoC},k_T,k_I}(SoC, T, i)\,(1 - a_j) i(k), \quad j = 1,2,\ldots,n_{RC},$$

$$v(k) = OCV(k) + \sum_{k_{SoC}=1}^{n_{SoC}} \sum_{k_T=1}^{5} \sum_{k_I=1}^{2} R_{0,k_{SoC},k_T,k_I} f_{k_{SoC},k_T,k_I}(SoC, T, i)\, i(k) + \sum_{j=1}^{n_{RC}} v_j(\mathrm{k}) \tag{10}$$

In order to ensure smooth parameter transition between temperature levels, constraints are applied to ensure that the resistor values decrease monotonously with temperature increasing.

$$R_{j,k_{SoC},k_T,k_I} \;\geq\; R_{j,k_{SoC},k_T+1,k_I}, \;\; j = 0,1,\ldots,n_{RC}, k_{soc} = 1,2,\ldots,n_{SoC}, k_T = 1,2,3,4, k_I = 1,2$$

Further, according to the Bulter-Volmer equation, the battery resistance also decreases as the current increases. Therefore, the following constraints are introduced,

$$R_{1,k_{SoC},k_T,1} \;\geq\; R_{1,k_{SoC},k_T,2}, \;\; k_{soc} = 1,2,\ldots,n_{SoC}, k_T = 1,2,3,4,5$$

Note that once the values of the RC time constants τ_j, $j = 1,2,\ldots,n_{RC}$ are set, the resistor values of the 3D look-up table, R_{j,k_{SoC},k_T,k_I} are all linear parameters. These linear parameters can be optimized using least squares method which guarantees global optimum and high efficiency. On the other hand, the nonlinear parameters τ_j, can be optimised using a global optimisation algorithm. In this paper we use three RC networks, i.e., $n_{\mathrm{RC}} = 3$. With only three nonlinear parameters to optimize, the chance of finding global minimum is greatly increased compared with optimizing all the model parameters (τ_j and R_{j,k_{SoC},k_T,k_I}) together using e.g., Genetic algorithm [3].

The rest steps to optimise the resistor values and the time constants are similar to that shown in [3], [4]. Therefore, it is not elaborated here. The final parameter optimisation procedure is shown in Figure S 2. The Matlab function 'lsqlin' was used as the least squares solver to optimise the linear parameters R_{j,k_{SoC},k_T,k_I}, and the Matlab function 'fmincon' was used to optimise the nonlinear parameters τ_j.

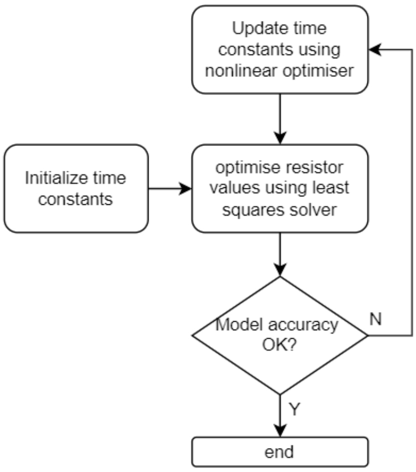

Figure S 2 the parameter optimisation procedure.

Test data

The test data used for model parameter optimization are summarized in Table S 1. The test data are illustrated in figures below.

Table S 1 Test data used for model parametrisation

Current profile	**Temperature levels**
1C pulse discharge test (pulse width 4% SoC)	[15, 25, 35, 45, 55] °C
1C CC discharge test	[25, 35, 45] °C
2C pulse test (pulse width 4% SoC)	[25, 35, 45] °C
2C pulse test (pulse width 4% SoC)	[25, 35, 45] °C
2C pulse test (pulse width 4% SoC)	[25, 35, 45] °C

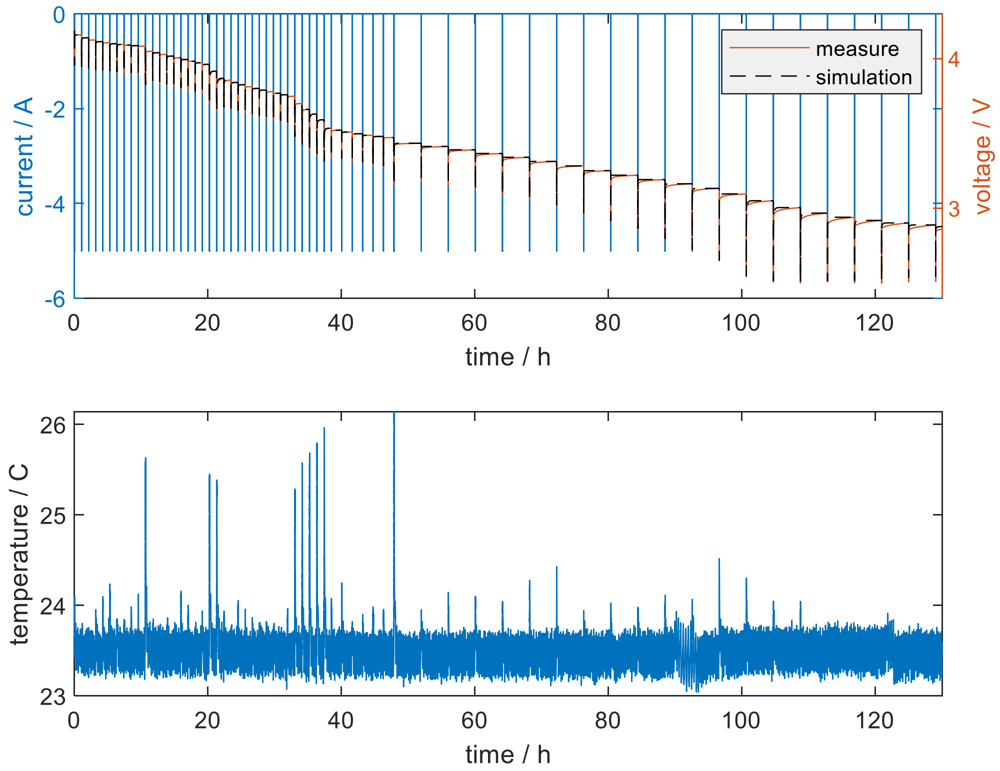

Figure S 3 Battery pulse discharge test data at 1C under 25 °C, and the voltage simulation results of the model

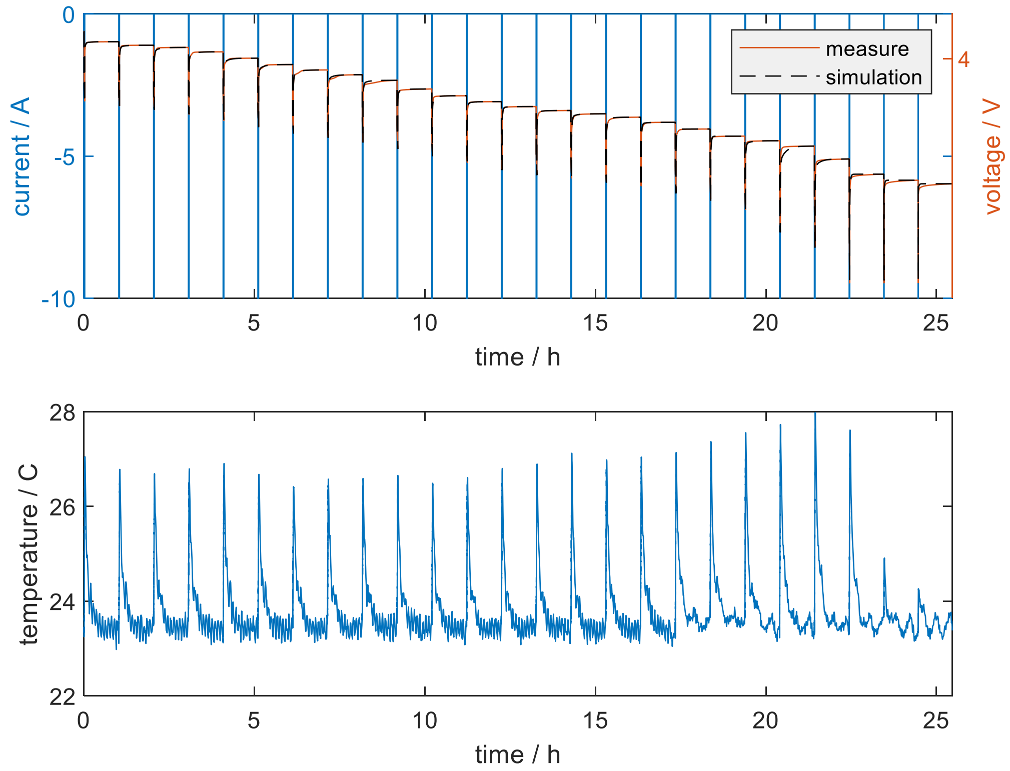

Figure S 4 Battery pulse discharge test data at 2C under 25 °C, and the voltage simulation results of the model

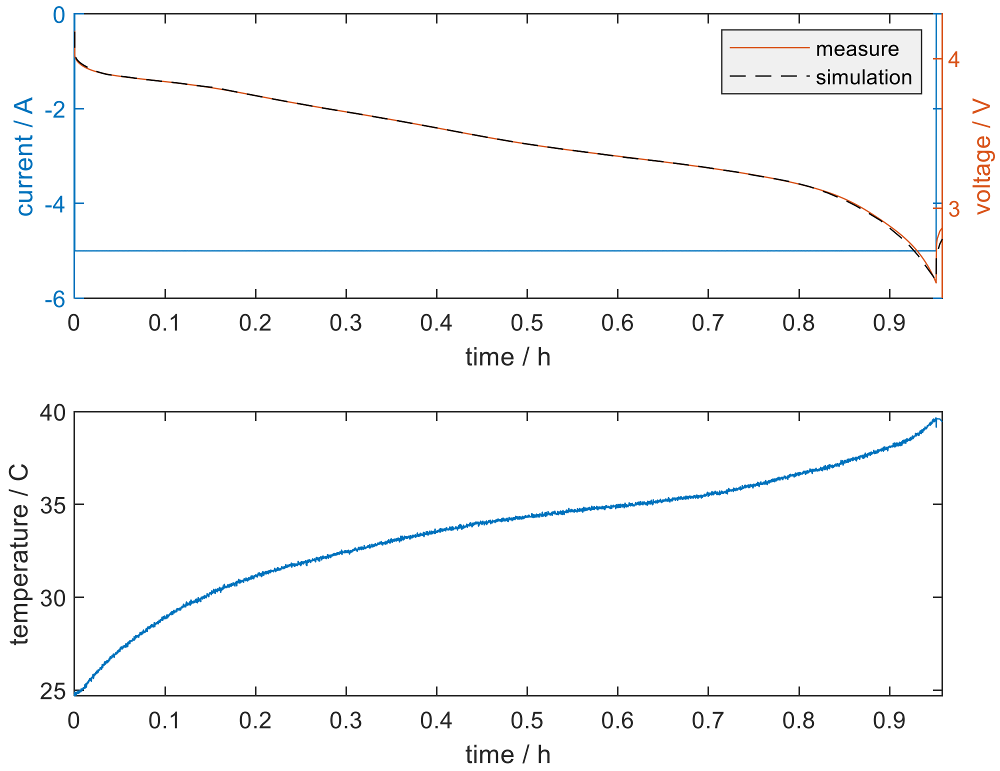

Figure S 5 Battery CC discharge test data at 1C under 25 °C, and the voltage simulation results of the model

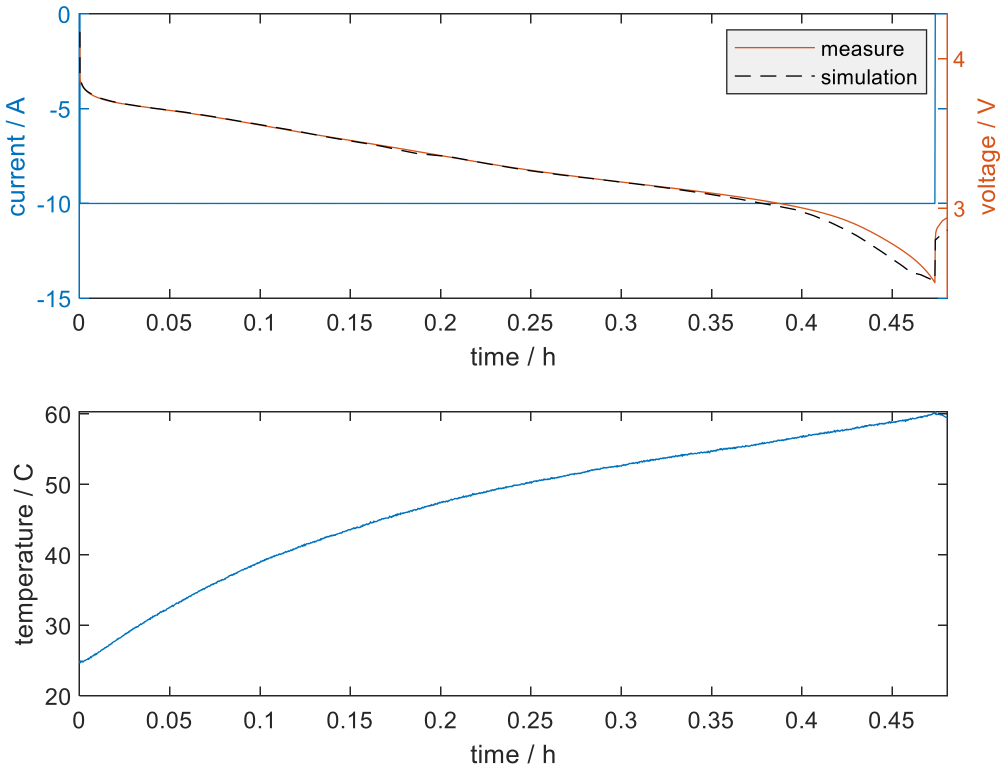

Figure S 6 Battery CC discharge test data at 2C under 25 °C, and the voltage simulation results of the model

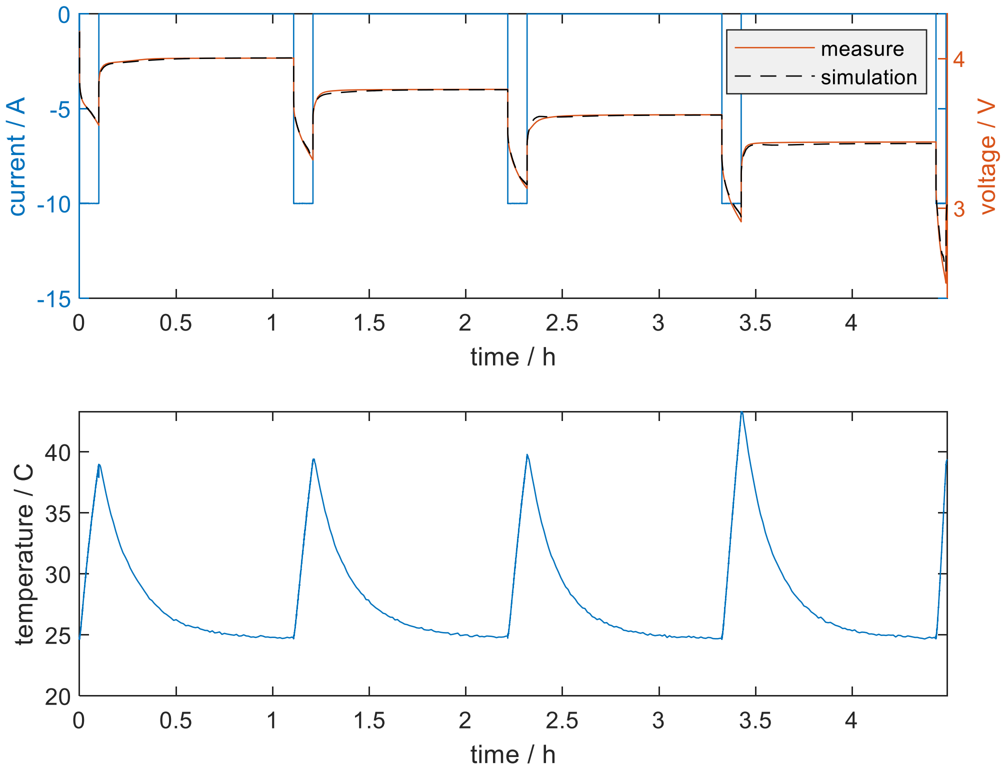

Figure S 7 Battery pulse discharge test data at 2C under 25 °C. Each pulse reduces the battery's SoC by about 20%.

Reference

[1] C. Zhang, K. Li, L. Pei, and C. Zhu, "An integrated approach for real-time model-based state-of-charge estimation of lithium-ion batteries," *J. Power Sources*, vol. 283, pp. 24–36, 2015.

[2] C. Zhang, K. Li, J. Deng, and S. Song, "Improved Realtime State-of-Charge Estimation of LiFePO4 Battery Based on a Novel Thermoelectric Model," *IEEE Trans. Ind. Electron.*, vol. 64, no. 1, pp. 654–663, 2017.

[3] C. Zhang *et al.*, "A new design of experiment method for model parametrisation of lithium ion battery," *J. Energy Storage*, vol. 50, p. 104301, 2022, doi: https://doi.org/10.1016/j.est.2022.104301.

[4] S. Li *et al.*, "Optimal cell tab design and cooling strategy for cylindrical lithium-ion batteries," *J. Power Sources*, vol. 492, p. 229594, 2021, doi: https://doi.org/10.1016/j.jpowsour.2021.229594.